An Exact Analysis for Freeze-out and Exhaustion in Single Impurity Semiconductors

Ron J. Pieper, Sherif Michael
Department of Electrical Engineering/ Department of Electrical and Computer Engineering
University of Texas, Tyler/ Naval Postgraduate School
Tyler, TX 75799/ Monterey, CA 93943

Introduction

In this paper, a complete analytical description for an exact expression for temperature dependence of the majority carrier in a single-impurity, equilibrium semiconductor is proposed. Analysis establishes that the problem is solvable exactly by identifying the only physically possible root to a cubic equation. This model provides an attractive alternative to approximate standard classroom approaches for this topic covered in senior and first year graduate level solid state courses in physics and electrical engineering.

Integrated circuits (ICs) are specified to operate between designated temperature limits. The circuit designer selects the doping level or levels and typically assumes that the dopants are approximately 100% ionized, i.e., exhaustion of dopant and the temperature is not too high. There can be a significant impact on the values for a plethora of device parameters, such as depletion width or a field effect transistor (FET) threshold voltage, if the assumption is violated. If the temperature is too low, the percentage ionization of dopant or dopants will be significantly less than 100%. This reversal of the high percentage of ionization of the dopant is commonly referred to as freeze-out. Most semiconductor devices and ICs are designed to be operated in exhaustion regime also known as "extrinsic regime" see Figure 1, borrowed from B. Streetman's classic undergraduate text book[1] , for which the majority carrier concentration is approximately equal to the dopant concentration e.g. $N_D=10^{15}/cm^3$. Again, in reference to Fig. 1, if the temperature is too high, the thermal generation effect causes the majority carrier concentration to become excessively higher than the dopant in what is called the intrinsic temperature regime. In the intrinsic regime, the majority carrier concentration is approximately the intrinsic concentration, n_i. The exhaustion regime lies between theses two extremes, intrinsic and freeze-out. The semiconductor designer will be interested in the temperature dependence of the majority carrier. As on Fig. 1, this dependence is often represented as a log-plot of the majority carrier concentration versus reciprocal of the temperature, T.

A simplified three regime model for the principal features observed on Fig. 1 is represented on Figure 2 with identifiable graphical guidelines[2,3]. Validity of the guidelines rests on several assumptions the first of which is the semiconductor is singly doped. Additional assumptions placed on the semiconductor include spatial uniformity in the physical properties, compliance with the Boltzman Approximation and equilibrium[1,2,3], i.e., no external stimulus

and no significant evanescent transients. The boundaries of the exhaustion regime T_U and T_L, which appear on Fig. 2 , impact consideration involving temperature limits on the operation of ICs. The roll-off slope of the curve in freeze-out, a specified graphical guideline on Fig. 2, is proportional to an energy level δE, the acceptor energy level for P-type dopant, or donor energy level, for N-type dopant[2,3]. Figure 3, shows a band diagram. As indicated on Fig. 3, the valence band edge serves as a convenient reference level to measure electron energy and identify acceptor and donor energy levels. If the Fermi energy level does not come within 3kT, as identified on Fig. 3, of either the conduction band edge, E_C, or valence band edge, E_V, the Boltzman approximation is assumed to be valid[1,3].

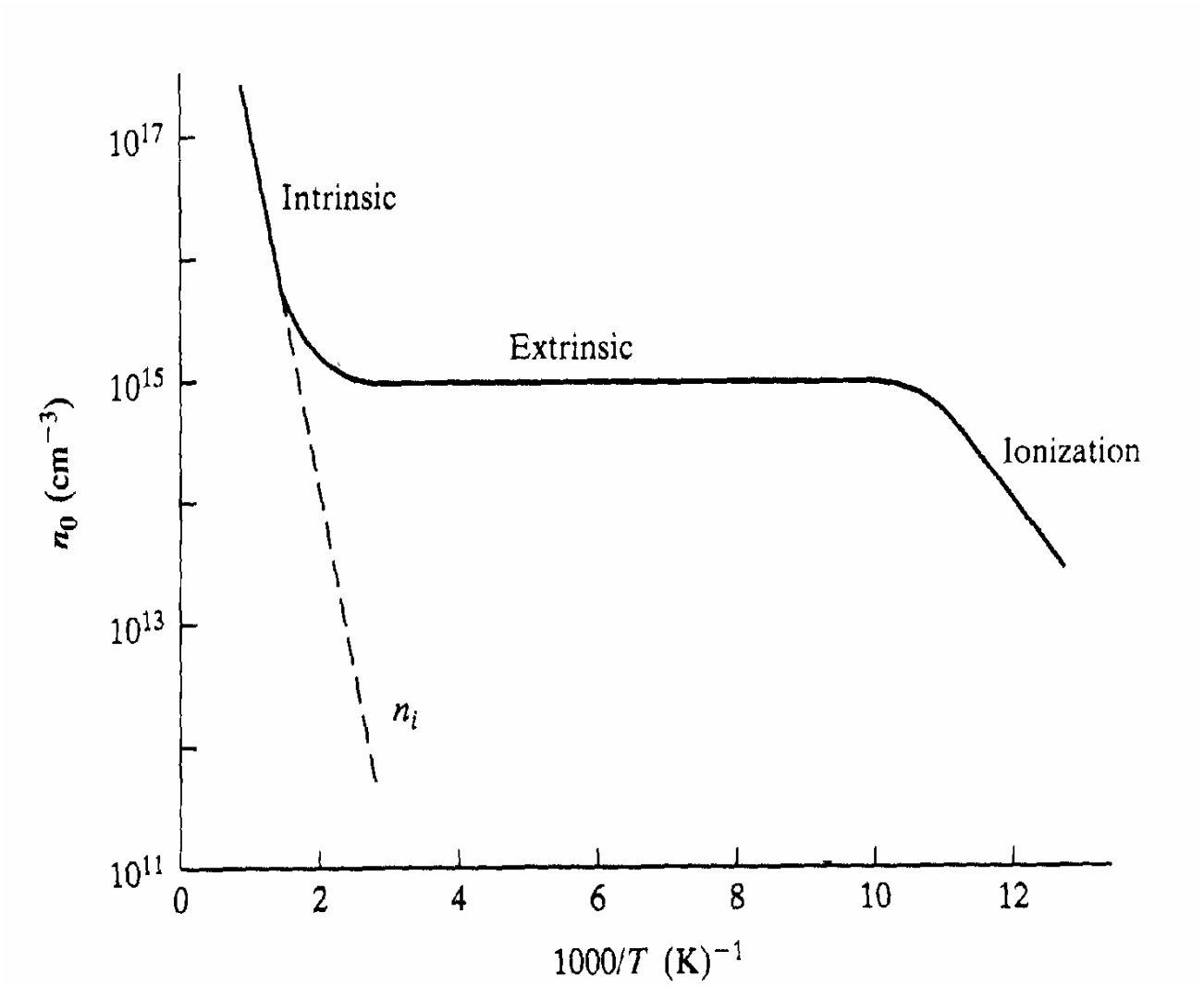

Figure 1. "Carrier Concentration vs. inverse temperature for Silicon doped with 10^{15} donors/cm^3" Figure and caption taken from Reference 1 for illustration purposes.

Significant background material has been summarized in Table 1, which covers independent variables and physical constants, and Table 2, which summarizes the dependent variables and related equations involving dependent and independent variables.

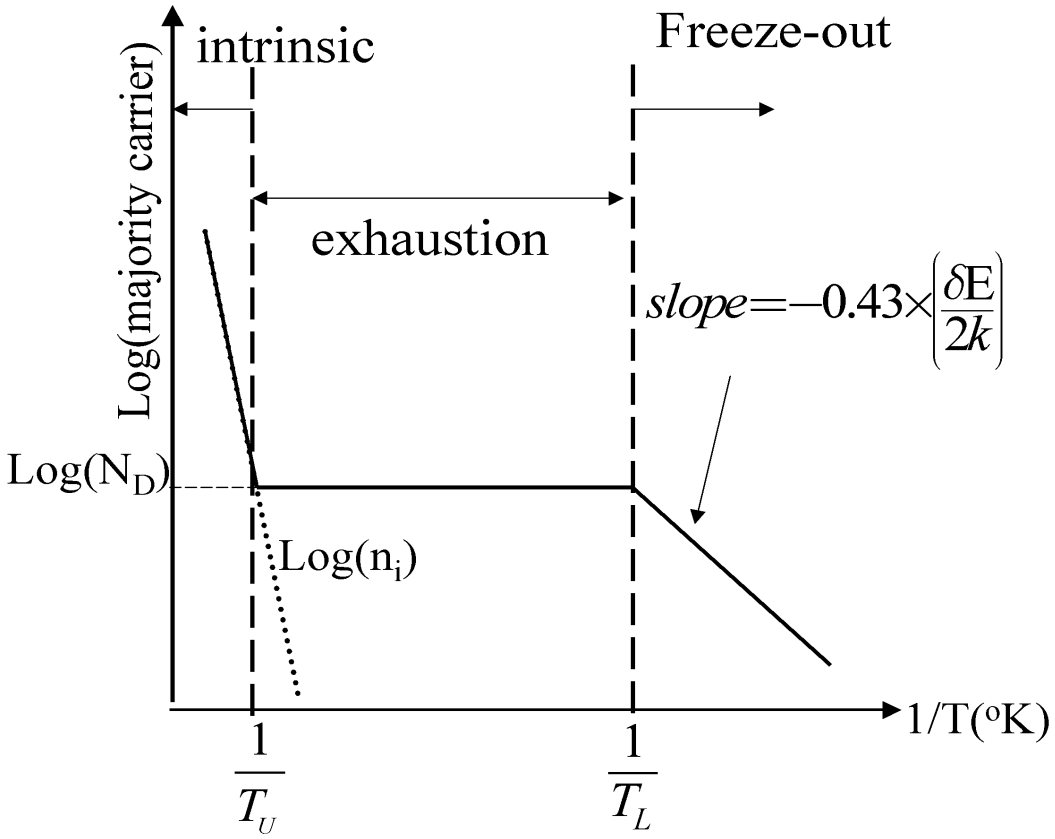

Figure 2: Simplified temperature dependence for majority carrier concentration in singly doped semiconductor.

To date there are a number of approximate prediction methods for determining dominant features in plots such as Fig. 1. The original method, accredited to W. Shockley, is to find the Fermi energy level using a graphical approach which is can then be used to predict the the majority carrier concentration with a fairly straight-forward calculation[4]. Due to space limitations it is impossible to list all other methods. One scheme briefly described in Appendix A involves iterative solutions[3,5] for T_U and T_L. The iterative "rules" that were employed with the computer tests for this work and are summarized without proof[3,5] in the appendix of this paper.

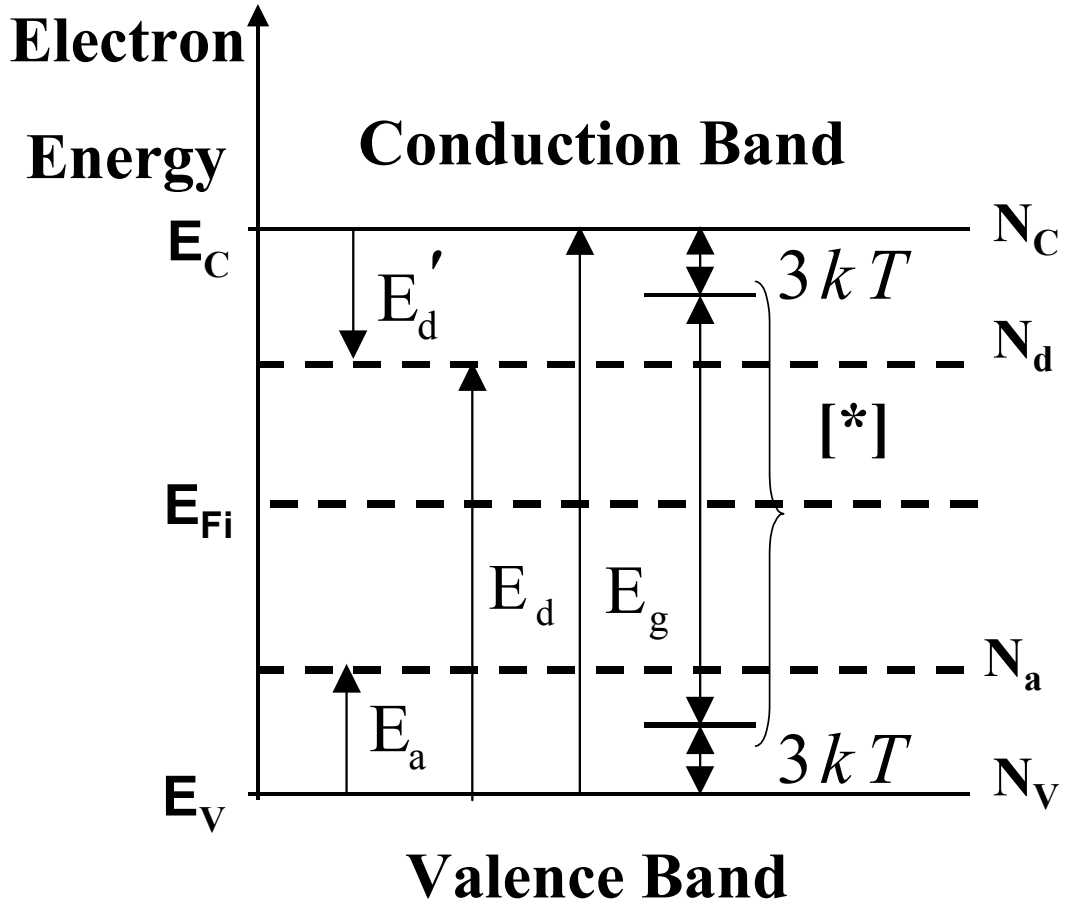

Fig 3 Band Diagram Parameters, Bracket identifies [*]Allowed Range E_F consistent with Boltzman Approximation

Introduced in this paper is an analysis treating all three temperature regimes shown on Fig. 1 in a comprehensive manner. The details of the solution involve extracting the physically correct root of a cubic polynomial equation. This analytic solution was recently checked for both materials Silicon and GaAs with a MATLAB based finite difference numerical algorithm[6].

General Analysis

The analysis begins with the general local charge neutrality equation,

$$p_o - n_o - \sum_{l=1}^{M_a} N_{a_l}^- + \sum_{l=1}^{M_d} N_{d_l}^+ = 0 \qquad (1)$$

for the special case in which there is only one impurity dopant. As defined in Table 1 this corresponds to either $M_a = 1$ and $M_d = 0$ or $M_d = 1$ and $M_a = 0$. The charge neutrality (1) is

based on observations that positively charged holes and negatively charged electrons in a semiconductor are also present with immobile, negatively ionized acceptors, and positively ionized donors. Explicitly examined in detail will be the case $M_d = 0$ and $M_a = 1$, i.e., P-type single impurity; however, the extension of the ideas to single impurity N-type semiconductor will be clarified.

Table 1: Independent Parameters and Physical Constants

Symbol	Description
M_a	Number of acceptor impurities
M_d	Number of donor impurities
m_p^*	Effective mass of holes
m_n^*	Effective mass of electrons
N_a	Concentration of acceptor dopant
N_d	Concentration of donor dopant
E_a	Acceptor energy level, see Fig. 3
E'_d	Donor energy level, see Fig. 3
E_g	Energy of the gap
g_a	Acceptor ground state degeneracy (4 typical for Silicon [1)
g_d	Donor ground state degeneracy (2 typical for Silicon [1)
T	Temperature (in Kelvin)
k	Boltzman Constant
m_o	Electron mass
h	Planck's Constant

The approach presented is facilitated by defining the parameter Z where

$$Z \equiv \exp\left[\left(E_{Fi} - E_F\right)/kT\right]. \tag{2}$$

From equilibrium electron and hole concentrations in Table 2 (lines 5 and 6),

$$n_0 = \frac{n_i}{Z} \tag{3a}$$

$$p_0 = n_i Z \tag{3b}$$

which, when combined with the local charge neutrality condition (1) and Table 2 (lines 10 and 11) substitutions leads to

$$0 = Z + \sum_{l=1}^{M_d} \frac{\overline{N}_{d_l}}{1 + K_{d_l} Z^{-1}} - Z^{-1} - \sum_{l=1}^{M_a} \frac{\overline{N}_{a_l}}{1 + K_{a_l} Z}, \tag{4}$$

where the temperature dependent factors,

$$K_{d_l} \equiv g_d e^{\left(E_{Fi} - E_{d_l}\right)/kT} \tag{5a}$$

and

$$K_{a_l} \equiv g_a e^{\left(E_{a_l} - E_{Fi}\right)/kT}, \tag{5b}$$

are needed to characterize partial ionization of donors and acceptors, respectively.

Table 2: Dependent Variables and Related Equations

Dependent Variable and/or Equation	Description(line #)
$N_C = 2(2\pi m_n^* kT)^{3/2}/h^3$	Conduction band density of states (1)
$N_V = 2(2\pi m_p^* kT)^{3/2}/h^3 = N_c\left(m_p^*/m_n^*\right)^{3/2}$	Valence band density of states (2)
$n_i = \sqrt{N_C N_V}\ \exp\left\{-E_g/(2kT)\right\}$	Intrinsic concentration (3)
$E_{Fi} = \frac{E_C + E_V}{2} + kT\ \ln\left(\frac{N_V}{N_C}\right) = \frac{E_g}{2} + kT\ \ln\left(\frac{N_V}{N_C}\right)$	Intrinsic Fermi Level (4)
$n_o = N_C \exp\{(E_F - E_C)/kT\} = n_i \exp\{(E_F - E_{Fi})/kT\}$	Equilibrium concentration of electrons (5)
$p_o = N_V \exp\{(E_V - E_F)/kT\} = n_i \exp\{(E_{Fi} - E_F)/kT\}$	Equilibrium concentration of holes (6)
$n_o p_o = n_i^2$	Law of Mass-action (7)
$N_d^+ = N_d/[1 + g_d \exp\{(E_F - E_d)/kT\}]$	Concentration of ionized donors (8)
$N_a^- = N_a/[1 + g_a \exp\{(E_a - E_F)/kT\}]$	Concentration of ionized acceptors (9)
$\overline{N}_a \equiv N_a/n_i$	Normalized acceptor concentration (10)
$\overline{N}_d \equiv N_d/n_i$	Normalized donor Concentration (11)
$E_d = E_C - E_d' = E_g - E_d'$	Donor level as defined Figure 3(12)

The specified problem of interest here is a single impurity dopant arbitrarily taken to be P-type. This special case corresponds to $M_a = 1$ and $M_d = 0$ in (1) and to lighten the notation the subscripts required for the general case $M_a > 1$ and/or $M_d > 1$ will be dropped.

$$0 = Z - Z^{-1} - \frac{\overline{N}_a}{1 + K_a Z} \quad . \tag{6}$$

This equation serves as the starting point for the next section.

Exact Analytical Solution (Single Impurity)

Algebraic manipulation of Eq. (6) , leads to a cubic equation in *Z*.

$$Z^3 + \frac{1}{K_a} Z^2 - \left(1 + \frac{\overline{N}_a}{K_a}\right) Z - \frac{1}{K_a} = 0 \ . \tag{7}$$

The corresponding result for a single impurity N-type is exactly the same form, producing a cubic in $Y = 1/Z$ with revised coefficients obtained by letting the '*a*' subscript (for acceptor) be replaced with the '*d*' subscript (for donor). The solution to (7) can be defined in terms of coefficients of the reference cubic equation.

$$Z^3 + a_1 Z^2 + a_2 Z + a_3 = 0, \tag{8}$$

where, by comparison of (7) and (8)

$$a_1 = \frac{1}{K_a} > 0 \ , \tag{9a}$$

$$a_2 = -\left(1 - \frac{\overline{N}_a}{K_a}\right) < 0 \ , \tag{9b}$$

and

$$a_3 = -\frac{1}{K_a} < 0 \ , \tag{9c}$$

where K_a and $\overline{N}_a$ are defined by (5b) and Table 2 (line 10), respectively.

After noting exactly one sign variation across the coefficients of (8), i.e., Sign $\{(1, a_1, a_2, a_3)\}$ = (+,+,- ,-), an application of Descartes' Rule of Signs[7] guarantees that there will be one and only one positive root for (8). As per the Fundamental Theorem of Algebra there will be a total of three roots. To facilitate representation of the solution to a cubic equation the following intermediate parameterization of coefficients[8] is taken ,

$$Q = (3a_2 - a_1^2)/9 \ , \tag{10a}$$

$$R = (9a_1 a_2 - 27a_3 - 2a_1^3)/54 \ , \tag{10b}$$

and

$$D \equiv Q^3 + R^2 \ . \tag{10c}$$

The "discriminant factor", for the cubic polynomial *D*, will dictate the type of solutions possible[8]. For *D* negative, all roots are real; while for *D* positive, only one root is real while the other two are complex. If *D* is zero, there will be repeated roots. Using symbolic mathematical methods, one can show, through substitution of (9) into (10), both Q and D are negative.

$$D = -\frac{1}{27}\{(1-\frac{1}{K_a^2})^2 + \frac{3\overline{N}_a^2}{K_a^2} + \frac{\overline{N}_a^3}{K_a^3} + \frac{5\overline{N}_a}{K_a^3} + \frac{\overline{N}_a^2}{4K_a^4}\} < 0 \qquad (11a)$$

and

$$Q = -\frac{1}{3}\{1 + \frac{\overline{N}_a}{K_a} + \frac{1}{3K_a^2}\} < 0. \qquad (11b)$$

The desired positive to root for cubic equation (8), for $D < 0$, is predicted by the cubic solution recipe[8].

$$Z = 2\sqrt{-Q}\cos(\theta/3) - \frac{1}{3}a_1 \ , \qquad (12a)$$

where

$$\theta = \cos^{-1}\left(R/\sqrt{-Q^3}\right) . \qquad (12b)$$

The other two solutions to the cubic (16), with $D < 0$, are obtained via (12a) after the substitution, $\theta/3 \rightarrow (\theta/3 + i\times 120^0) \quad i = \pm 1$, and are identifiable as the two negative *nonphysical* solutions to (8). The prediction for Z with n_i in Table 2 (line 3) can then be used with (3b) to predict *exact* temperature dependent majority carrier concentration, p_o.

Table 3: Parameters Used in Tests

Parameter	Value
E_a	0.05 eV
N_a	10^{13} ,10^{15}, 10^{17} #/cm^3
E_g	1.11 eV (Silicon)
m_p^*	$0.56m_o$
m_n^*	$1.1m_o$
g_a	4 (Silicon)

MATLAB Computer Test

Table 3 identifies values for the independent parameters selected for the demonstration of the concepts and solutions previously introduced. On Fig. 4 three plots appear using the three-regime, exact analytic solution obtained as described at the end of the previous section. Independent parameter values from Table 3 were taken. Each of these curves has the characteristic shape as depicted in Fig 1. The conclusion from Fig. 4 is that lighter doping leads to the onset of freeze-out at lower temperatures. Also, one should note relatively short vertical markers, two lines per curve, which cut the curves at transitions into what is recognized as freeze-out and intrinsic regimes. The temperatures that were used to "place" the markers on these curves were obtained from the limit values from the iterative rules in Appendix A.

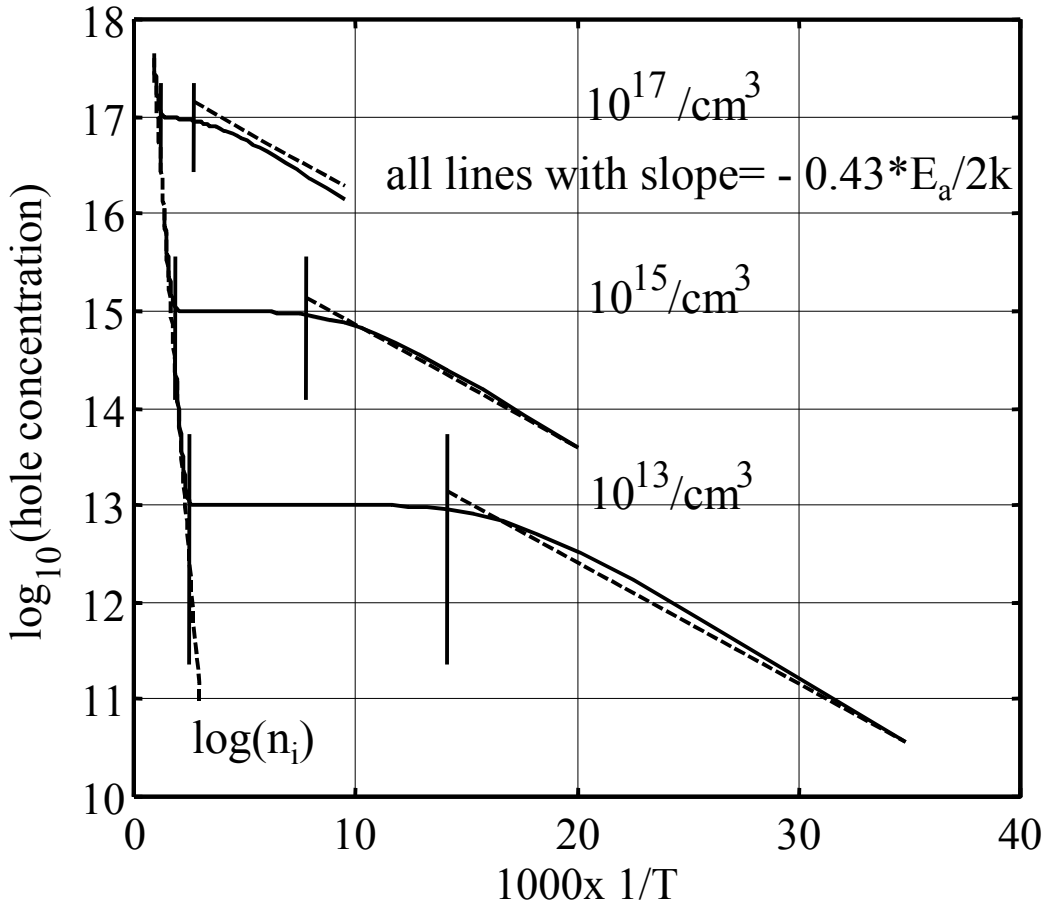

Figure 4 Exact solution for log ($p_o(T)$), vertical (solid) lines at T_U and T_L, and tests for graphical guidelines (dashed).

On Fig. 4, one should observe an approximately linear, dashed curve labeled log (n_i). This curve was obtained by plotting the base-10 logarithm of the intrinsic concentration, Table 2. Alignment between log (n_i) curve and the intrinsic regimes curves for exact analytic solution for log (p_o) is seen to be fairly close for each doping level case. For each of the doping levels identified in Table 3, the overlay between the corresponding freeze-out part of the curve and dashed lines in the freeze-out part of the curves is approximately correct, as displayed on Fig 4. The level of agreement in slopes supports the freeze-out regime graphical guideline depicted on the RHS (right hand side) of Fig 2.

"Hands On" Student Test

Students in the current (Spring 05) offering of Solid State Electronics class (EE4350) at UT Tyler Texas, were asked to determine, using the MATLAB computer code for the model described herein, the temperature boundaries of "operation" of a (PNP) bipolar junction

transistor (BJT) . It should be pointed out that not all solid state texts (including Streetman's text [1]) provide a *quantitative model* for predicting upper and lower temperature domain edges evident from curves showing up in Fig 2. The students were instructed to consider a typical transistor design where emitter is doped is doped much higher than base or collector domains [1]. For a specific Silicon PNP BJT design the emitter is doped P-type impurity Boron with concentration $N_a = 1.0\times10^{16}\,cm^{-3}$ and acceptor energy level $E_a = 0.045$ eV, the base is doped N-type impurity Phosphorous with concentration $N_d = 1.0\times10^{14}\,cm^{-3}$ with donor energy level $E_d = 0.044$ eV, and the collector is doped P-type impurity Boron with $N_a = 11.0\times10^{15}\,cm^{-3}$ and acceptor energy level $E_a = 0.045$ eV. The program the students use require them to eventually guess reasonable temperature limits for display of majority carrier concentration but a bad guess is easily corrected thru trial and error. The estimated boundaries for device operation are determined by the following conservative guideline. The upper temperature boundary (T_U) is where the majority concentration is 110% of the doping level. The lower temperature boundary (T_L) is where the majority carrier concentration is 90% of the doping level. The location for the temperature boundaries will correspond to "eye-ball" estimated bends in the curves (see Figs 1, 2, 4). This estimation process can easily be made more precise by a little additional programming but the main point is the same. The estimated boundaries for the example described above are summarized in Table 4.

Table 4. Expected Data for Student Experiment

Doping Level (type)	T_U (^oK)	T_L (^oK)	(T_U (^oK)- T_L)(^oK)
10^{16} cm^{-3} (P)	660	190	470
10^{14} cm^{-3} (N)	460	85	375
10^{15} cm^{-3} (P)	550	120	430

The simulation experiment will require the student to draw some conclusions from the extracted data. First, despite appearances from the majority carrier concentration curves plotted versus reciprocal temperature (see Fig 4) the data seen in 3rd column of Table 4 correctly suggests that the temperature span is fairly constant and not shrinking dramatically with increases in doping. At this point it is expected that the student can and will interpret the limitations suggested by Table 4. Because all three regions of the transistor need to remain within their respective boundaries it is correct that the lowest of the upper limits T_U in Table 4 will determine the overall upper limit of operation. ($460^oK = 187^0C$). Similarly, the highest of the lower limits T_L in Table 4 will determine the overall lower limit of operation. ($190\ ^oK = -83^0C$). Therefore the student concludes that the operation range for the transistor specified becomes [-83^0C, to 187^0C]. To drive home the relevance of the simulation experiment the instructor can provide a specification sheet for a *typical* PNP transistor. For example the 2N3906 PNP small signal transistor has the specified operating temperature range [-55^0C, to 150^0C]. Due to fair agreement between specified temperature limits and the data produced from the simulation experiment the student may well ask if there are other factors to consider. The answer is yes. Besides the temperature dependence of the majority carrier discussed in this paper it is known that high temperature carrier transport

effects, which can lead to "thermal runaway" in transistors, are considered by the manufacturer when publishing recommended temperature limits of operation.

Conclusions

A comprehensive analytic approach to solving and displaying the characteristic curve describing the freeze-out, intrinsic, and exhaustion regimes has been derived and tested. The relatively new methods discussed here would serve as an attractive alternative or supplement to the currently employed classroom approaches. These more traditional approaches include graphical methods, patch-work solutions, and iterative computation. The solution discussed in this paper for the three-regime, comprehensive, analytical solution is simple enough that students can easily test the concepts by implementing them with a few lines of code on any of the commercially available mathematical packages. An example based on a bipolar transistor was explored in this paper and results were supported by the data taken from a specification sheet for a commonly used PNP transistor. This example, was included to clarify to the student the significant role played by this phenomena in determining the recommended temperature limits of solid state semiconductor devices.

References

[1] Ben G. Streetman and Sanjay Banerjee, Solid state Electronic Devices, 5th Edition, Prentice Hall, 2000, text book selected for use at U.T. Tyler undergraduate electrical engineering course in solid state devices, Spring 2005

[2] B. Sapoval and C. Hermann, *Physics of Semiconductors*, Springer Verlag, New York, 1995, p. 105

[3] Ron J. Pieper and Sherif Michael**,** "Comprehensive Approach to Predicting freeze-out and exhaustion in uniform single impurity Semiconductors in Equilibrium", *IEEE Transactions on Education*, A*ccepted for publication*

[4] W. Shockley, *Electrons and Holes in Semiconductors*, D. Van Nostrand, Princeton, N.J. 1950.

[5] A. Bar-Lev, *Semiconductor Electronic Devices*, 3rd Edition, Prentice Hall, 1993, p. 93.

[6] R. Pieper, S. Michael, and D. Reeves, "Comparison of Analytic and Numerical Models with Commercially Available Simulation Tools for Prediction of Semiconductor Freeze-out and Exhaustion," Invited paper presented at the *45th Midwest Symposium on Circuits and Systems*, Tulsa OK, Aug. 5-7, 2002.

[7] A. D. Kraus, *Matrices for Engineers,* Oxford University Press, New York, 2002.

[8] M. Spiegel and J. Liu, *Schaum's Outline Series, Mathematical Handbook of Formulas and Tables*, McGraw-Hill, New York, 1999.

RON J. PIEPER

Ron J. Pieper is currently an Associate Professor with the Department of Electrical Engineering at the University of Texas, Tyler. He received the B.S. degree in physics from the University of Missouri, St. Louis, in 1974, the M.S. degree in physics and the M.S. degree in electrical engineering from the University of Wisconsin, Madison, in 1976 and 1979, respectively. In 1984, he received the Ph.D. in electrical and computer engineering from the University of Iowa, Iowa City. Dr. Pieper is a senior member of IEEE and a member of ASEE. He is also a registered Professional Engineer in the state of Virginia. His research interests include engineering optics and image processing.

SHERIF MICHAEL

Sherif Michael received his B.S.E.E., M.S.I.E. & Ph.D. degrees in 1974, 1980 and 1983, respectively. He joined the Department of Electrical and Computer Engineering at the Naval Postgraduate School, Monterey CA, in 1983. He is also a member of the Space System Group since its initiation in 1985. His present research is in the area of

analog and digital signal processing, Mixed-Mode VLSI, design of spacecraft power systems, and radiation effects on semiconductor devices, including annealing of solar cells and the design of radiation-hardened devices. In over 21 years as a faculty member at NPS, he has served as thesis advisor for more than 70 ECE/Space students. He has more than 75 technical publications in professional Journals and International Conferences. He organized and chaired the 1998 IEEE International Symposium on Circuits and Systems, in Monterey, CA. He also organized and chaired the 34th Midwest Symposium on Circuits and Systems, in Monterey, CA, in 1991. He is registered as a Professional Engineer and a senior member of IEEE.

Appendix Rules for Iterative Prediction of T_U and T_L

Algorithms for iterative prediction of these temperatures, depicted on Fig. 2, are presented here without the "proofs", which are located elsewhere[3,5] in order to minimize the distraction for the reader. Because the temperature prediction rules involve temperature-dependent parameters, the approach requires iterative substitution until a "convergence" is reached. Both rules require a seed temperature to begin the iterative process. The rule for the upper temperature T_U is

$$T_U = \frac{E_g}{2k \ln\left\{\dfrac{\sqrt{N_C N_V}}{\sqrt{\delta_U^2 + \delta_U} N_a}\right\}}, \tag{A1}$$

where the fractional increase in the majority carrier over that associated with the exhaustion regime, δ_U, as defined by the relation

$$p_O = \left(1 + \delta_U\right) N_a. \tag{A2}$$

In the program simulations δ_U was set to 0.1, or equivalently 10% over 100% ionization.

A rule for predicting the lower temperature limit, T_L, is

$$T_L = \frac{E_a}{k \ln\left\{\dfrac{\delta_L N_V}{(1 - \delta_L)^2 g_a N_a}\right\}}, \tag{A3}$$

in which the fractional *decrease* in the majority carrier over that associated with the exhaustion regime, δ_L, is defined by the relation

$$p_o = (1 - \delta_L) N_a. \tag{A4}$$

In the program simulations δ_L was set to 0.1, or equivalently 10% diminished from 100% ionization. The data predictions for T_U and T_L were helpful in selecting an appropriate temperature range for plotting the three-regime, analytic solution.